Slip-flow boundary condition for straight walls in the lattice Boltzmann model

Lajos Szalmás
Faculty of Natural Sciences, Budapest University of Technology and Economics, Müegyetem rakpart 3-9, H-1111 Budapest, Hungary
(Received 3 February 2006; published 29 June 2006)

A slip-flow boundary condition has been developed in the lattice Boltzmann model combining an interpolation method and a simple slip boundary condition for straight walls placed at arbitrary distance from the last fluid node. An analytical expression has been derived to connect the model parameters with the slip velocity for Couette and Poiseuille flows in the nearly continuum limit. The proposed interpolation method ensures that the slip velocity is independent of the wall position in first order of the Knudsen number. Computer simulations have been carried out to validate the model. The Couette and Poiseuille flows agree with the analytical results to machine order. Numerical simulation of a moving square demonstrates the accuracy of the model for walls moving in both the tangential and normal directions.

DOI: 10.1103/PhysRevE.73.066710 PACS number(s): 02.70.−c, 05.10.−a, 05.20.Dd, 45.50.−j

I. INTRODUCTION

The lattice Boltzmann method is a powerful tool in modeling hydrodynamics and gas kinetics. Historically, it was developed from lattice gas automata, replacing the Boolean variables with continuous distribution functions at each lattice site to avoid noise effects [1]. Later derivations revealed that the method is a special discretization of the continuous Boltzmann equation [2].

An important issue of this kinetic nature is the way that special boundary conditions are imposed. In bounce-back methods particle populations leaving the computational domain are reflected from a real or hypothetical boundary node at the solid-liquid interface. It has been pointed out that the proper choice of such a boundary node (halfway wall) can ensure second-order accuracy in space for some simple flows [3,15]. On the other hand several attempts have been made to improve the bounce-back scheme for arbitrary boundaries, for example using volumetric methods [4] or interpolation techniques [5].

Recently, the lattice Boltzmann method has been applied to microfluid applications [6–9]. In this case the fluid dynamics differ from the conventional hydrodynamics. As the mean free path becomes comparable with the characteristic device size, a noticeable slip appears over the solid-liquid interface. Similar behavior can be observed in rarefied gas flows [10]. Although at higher Knudsen number (the ratio of the mean free path and the macroscopic size) the continuous description is no longer valid, the lattice Boltzmann method can provide accurate results with its kinetic nature. It is clear that boundary conditions applied to this phenomenon should rely on kinetic background. Several authors use modified bounce-back schemes taking into account reflecting and specularly reflecting particles with different boundary treatments to ensure the slip condition at the wall [7,9,11]. Tang *et al.* have established a discrete version of the general Maxwell-type boundary condition [8]. All these schemes are restricted to simple geometries, to flat walls placed at a definite position related to the fluid nodes.

In this paper we present a modified interpolation method which is able to model the slip-flow boundary condition for straight walls placed at an arbitrary position. The proposed boundary rules ensure that the slip length is independent of the wall position. The model is based on the kinetic background; the unknown distribution functions are determined using the scattering kernel, which involves reflecting and specularly reflecting interactions between the wall and the outgoing particles. The wall movement is taken into account by varying the incoming particle densities; we assume that the tangential momentum of the slipping particles does not change. An analytical formula is derived for Couette and Poiseuille flows, which connects the model parameters with the slip velocity; then computer simulations are carried out to examine the model in these cases. A moving square is also simulated, which demonstrates the accuracy of the method for walls moving in both the tangential and normal directions.

II. FORMULATION OF THE MODEL

A. Rules of the boundary condition

Our starting point is the lattice Boltzmann model with the single-relaxation-time approximation [12]. We choose to work in two dimensions on a square lattice. Let $f_i(\boldsymbol{x},t)$ be the particle distribution functions at site $\boldsymbol{x}$ at time t moving in the direction of $\boldsymbol{c}_i$, $i=0,\ldots,8$, where the speed vectors along the lattice links are $\boldsymbol{c}_0=\boldsymbol{0}$, $\boldsymbol{c}_i=\{\cos[\pi(i-1)/2],\sin[\pi(i-1)/2]\}$ for $i=1,2,3,4$ and $\boldsymbol{c}_i=\sqrt{2}\{\cos[\pi(i-\frac{9}{2})/2],\sin[\pi(i-\frac{9}{2})/2]\}$ for $i=5,6,7,8$.

The distribution functions evolve according to the lattice Boltzmann equation

$$f_i(\boldsymbol{x}+\boldsymbol{c}_i\delta,t+\delta)=\frac{\tau-1}{\tau}f_i(\boldsymbol{x},t)+\frac{1}{\tau}f_i^{eq}(\boldsymbol{x},t)+\rho g_i\delta. \quad (1)$$

Here, τ is the relaxation time, δ is the time (and lattice) step, and $f_i^{eq}(\boldsymbol{x},t)$ denotes the equilibrium distribution function for isothermal fluids given by Taylor expanding the Maxwellian distribution function up to second order,

$$f_i^{eq}=E_i\rho\left(1+3\boldsymbol{c}_i\boldsymbol{u}+\frac{9}{2}(\boldsymbol{c}_i\boldsymbol{u})^2-\frac{3}{2}\boldsymbol{u}^2\right), \quad (2)$$

where the weights are $E_0=4/9$, $E_i=1/9$ for $i=1,\ldots,4$ and $E_i=1/36$ for $i=5,\ldots,8$. The external forcing term is given

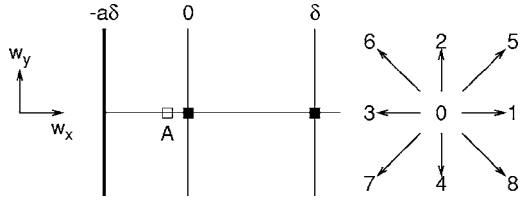

FIG. 1. Geometry of the solid-liquid interface and the nine-speed model, 3, 6, 7 as outcoming and 1, 5, 8 as incoming velocity directions relating to the wall. Filled squares represent fluid nodes, A is at half lattice spacing from the wall, and w_x, w_y denote the x, y components of the wall velocity.

by $g_i = 3E_i \boldsymbol{c}_i \boldsymbol{g}$, where $\boldsymbol{g}$ is the body force per unit mass. The macroscopic density and velocity are obtained by taking the moments of f_i,

$$\rho = \sum_i f_i, \tag{3}$$

$$\rho \boldsymbol{u} = \sum_i f_i \boldsymbol{c}_i. \tag{4}$$

Continuum hydrodynamic type equations modeled by this algorithm can be determined by performing the Chapman-Enskog procedure [13]. In the low-Mach-number approximation ($|\boldsymbol{u}| \ll c_s$) the continuity and the Navier-Stokes equation are recovered in $O(\delta^2)$; here $c_s = 1/\sqrt{3}$ is the speed of sound. Then the truncation error of the discretization is taken into account in the kinematic viscosity

$$\nu = \left(\tau - \frac{1}{2}\right) c_s^2 \delta. \tag{5}$$

Next we turn to introduce a moving boundary to the model. Let us consider a wall parallel to the y axis at an arbitrary position $x = -a\delta$. Figure 1 shows its position, the two neighboring fluid nodes used for the boundary condition, and the speed directions. After the streaming process the incoming particles are unknown on the links for $c_{xi} > 0$. The idea is that the outgoing particles with $c_{xi} < 0$ reflect from or slip on the wall. Two parameters r, s describe the weights of the reflecting and slipping particles; when $r = 1$ the total amount of particle density is reflected back. The sum of reflecting and slipping parts equals the total particle density; hence $r + s = 1$.

For moving boundaries a special treatment is needed to ensure momentum exchange between the separated phases. Ladd proposed to add a term to the incoming particle densities in proportion to the velocity of the boundary and the density in the cell; the method is developed from the lattice gas averaging of boundary-node collision rules [14]. Here, we assume that in the direction parallel to the wall only reflecting particles exchange momentum; slipping particles suffer zero friction during the collision. The unknown distribution functions at $x = 0$ are defined by the following rules:

$$f_1(0, t+\delta) = f_3^*(0,t) - \kappa f_3^*(\delta,t) + \kappa f_1(\delta, t+\delta) + \lambda 6 E_1 \rho w_x, \tag{6}$$

$$f_5(0, t+\delta) = s f_6^*(0,t) - s\kappa f_6^*(\delta,t) + r f_7^*(0,t) - r\kappa f_7^*(\delta,t) + \kappa f_5(\delta, t+\delta) + \lambda 6 E_5 \rho w_x + r\lambda 6 E_5 \rho w_y, \tag{7}$$

$$f_8(0, t+\delta) = r f_6^*(0,t) - r\kappa f_6^*(\delta,t) + s f_7^*(0,t) - s\kappa f_7^*(\delta,t) + \kappa f_8(\delta, t+\delta) + \lambda 6 E_8 \rho w_x - r\lambda 6 E_8 \rho w_y, \tag{8}$$

where $f_i^*(0,t), f_i^*(\delta,t)$ are postcollision functions at the boundary node and the nearest-neighboring fluid node governed by the right-hand side of Eq. (1), and w_x, w_y are the wall velocities in the x, y directions, respectively. In the above equations the weights κ, λ are given by

$$\kappa = \frac{2a - 1}{2a + 1}, \tag{9}$$

$$\lambda = \frac{2}{2a + 1}. \tag{10}$$

This method relies on the following approach. First, postcollision distribution functions are interpolated linearly using the information obtained from the first two fluid nodes at a fluid point A which lies at half lattice spacing from the wall. Second, during the streaming process these interpolated functions are used as outgoing particles collide with the wall and return to A as incoming particles. This collision embodies reflecting and specularly reflecting interactions, and momentum exchange caused by the wall movement. Third, unknown functions at the first fluid node are calculated using linear interpolation involving the incoming particles and the distribution functions at the second fluid node. It is shown below that this choice of the interpolation ensures that the slip length is independent of the wall position.

For $a = 0.5$, as a special case with fixed halfway position, the boundary conditions take the following form:

$$f_1(0, t+\delta) = f_3^*(0,t), \tag{11}$$

$$f_5(0, t+\delta) = s f_6^*(0,t) + r f_7^*(0,t) + r 6 E_5 \rho w_y, \tag{12}$$

$$f_8(0, t+\delta) = r f_6^*(0,t) + s f_7^*(0,t) - r 6 E_8 \rho w_y. \tag{13}$$

B. Derivation of the slip velocity for Couette and Poiseuille flows

In the following we apply the model to steady Couette and Poiseuille flows. In these cases all quantities are functions only of the x coordinate (we keep only this variable in the expressions), and $u_x(x) = 0$. Then a systematic analytical expression is derived to determine a presumed steady slip velocity over the wall. For this purpose, we calculate the y component of the momentum variation during the collision at the boundary. Since ρu_y contains pairs of f_i, we can simplify the calculation by introducing new variables such that

$$F_0(x) = f_2(x) - f_4(x), \tag{14}$$

$$F_1(x) = f_5(x) - f_8(x), \tag{15}$$

$$F_2(x) = f_6(x) - f_7(x). \tag{16}$$

Let us consider these variables at $x=0,\delta$. The velocities are denoted by $u_y(0)=u_0, u_y(\delta)=u_1$ and the body force is assumed to be along the y direction, $\mathbf{g}=g\mathbf{i}_y$. In this context the lattice Boltzmann equation Eq. (1) coupled with the momentum equation Eq. (4) can be solved exactly. The y components of the incoming and outcoming momentum pairs are obtained by

$$F_{1,2}(0) = \rho\left(\frac{u_0}{6} \mp \frac{\tau}{6}(u_1 - u_0) - \frac{2\tau^2}{3(2\tau-1)}g\delta + \frac{(2\mp 3)\tau}{6(2\tau-1)}g\delta\right), \tag{17}$$

$$F_{1,2}(\delta) = \rho\left(\frac{u_1}{6} \mp \frac{\tau}{6}(u_1 - u_0) - \frac{2\tau^2}{3(2\tau-1)}g\delta + \frac{(2\pm 3)\tau}{6(2\tau-1)}g\delta\right). \tag{18}$$

In these expressions u_0, u_1 are unknown quantities, which can be defined by assuming a particular flow profile in respect of Couette or Poiseuille flow. An additional constraint is the boundary condition Eqs. (7) and (8), which takes the following form:

$$F_1(0) = (1-2r)F_2^*(0) - (1-2r)\kappa F_2^*(\delta) + \kappa F_1(\delta) + r\lambda\frac{1}{3}\rho w_y, \tag{19}$$

where $F_i^*(x)$ are postcollision functions calculated from Eq. (1).

In the case of Couette flow $u_0=w_y+u_s+\alpha a\delta, u_1=w_y+u_s+\alpha(a+1)\delta$, where u_s is the extrapolated slip velocity at the wall, α is the velocity gradient, and $g=0$. Substituting Eqs. (17) and (18) into Eq. (19), after some algebraic manipulations, we obtain the slip velocity

$$u_s = \left(\tau - \frac{1}{2}\right)\frac{1-r}{r}\alpha\delta. \tag{20}$$

For Poiseuille flow $u_0=u_s+\alpha a\delta-\beta a^2\delta^2$, $u_1=u_s+\alpha(a+1)\delta-\beta(a+1)^2\delta^2$, $w_y=0$, and β is related to g via the Navier-Stokes equation $g=2\nu\beta$. Using these conditions, after the same calculation as in the case of Couette flow, we obtain that

$$u_s = \left(\tau - \frac{1}{2}\right)\frac{1-r}{r}\alpha\delta + \left(\frac{4\tau^2}{3} - \frac{5\tau}{3} + \frac{1}{2} - a^2\right)\beta\delta^2. \tag{21}$$

It is noticed that for the simple halfway bounce-back scheme ($a=0.5$, $r=1$) the same result is obtained [15].

III. NUMERICAL TEST

A. Steady Couette and Poiseuille flows

Computer simulations have been performed to compare the model with the theoretical calculation. Couette flow is modeled in an $N\times 1$ domain between two parallel walls; the left-hand side is placed at $x=-a\delta$ with $w_y>0$ and the right-hand side at $x=(N-1)\delta+a\delta$ with $w_y=0$. On both sidewalls the slip condition and on the top and bottom walls the periodic boundary condition is used. The initial position is chosen that $u_x=u_y=0$ and $\rho=1$ at each fluid node. The theoretical solution in the steady state is $u_x=0$ and u_y is a linear function of x. According to Maxwell's theory the slip velocity at the left and right walls is given by

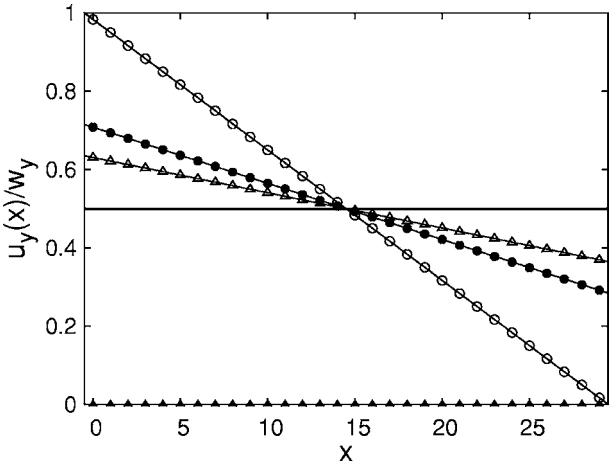

FIG. 2. Flow profile for Couette problem with halfway wall ($a=0.5$). Numerical results are plotted with empty circles for $\tau=1$, $r=1$, filled circles for $\tau=0.7$, $r=0.01$, empty triangles for $\tau=5$, $r=0.1$, and filled triangles for $\tau=1$, $r=0$. Analytical results are plotted with solid lines. Theoretical limit for $r\to 0$ crosses at $u_y(x)/w_y=0.5$.

$$\frac{u_s}{w_y} = \mp\frac{\xi}{2\xi + L}, \tag{22}$$

where ξ is the slip length. In our case $\xi=(\tau-0.5)\frac{1-r}{r}\delta$, and the channel width $L=(N-1+2a)\delta$. Figure 2 shows the simulated flow profiles in a 30×1 domain for different values of τ, r; the distance of the wall from the last fluid node is $a=0.5$. Points indicate the numerical results, which are in excellent agreement with the theoretical flow profiles. The extrapolated velocity at the wall u_w versus r can be seen in Fig. 3. The wall distance is $a=0.7$. It is clearly seen that when $r\to 0$ the velocity at the wall $u_w/w_y\to 0.5$ according to Eq. (22). $r=0$ is a singular point; the simulations give $u_y=0$ at all nodes. In this case all particles slip past the wall without momentum exchange. Several simulations have been carried out in wider domains ($N=60,120$), which give the same result; however, for the same τ, r the slip velocity is much lower, corresponding to Eq. (22). The velocity profile for Poiseuille flow simulated with the same domain size can be seen in Fig. 4. The analytical curves is plotted using the expression of the quadratic velocity profile with the constraint of channel symmetry. It is emphasized that the steady state results obtained from the simulations presented here are machine order accurate since Couette and Poiseuille flows are exact solutions in the lattice Boltzmann model [15].

In kinetic theory the slip velocity is considered as a function of the Knudsen number, which is $\mathrm{Kn}=c_s(\tau-0.5)/N$ in our case. It can be readily seen that the slip velocity obtained here shows clear dependence on Kn in first order. It can be

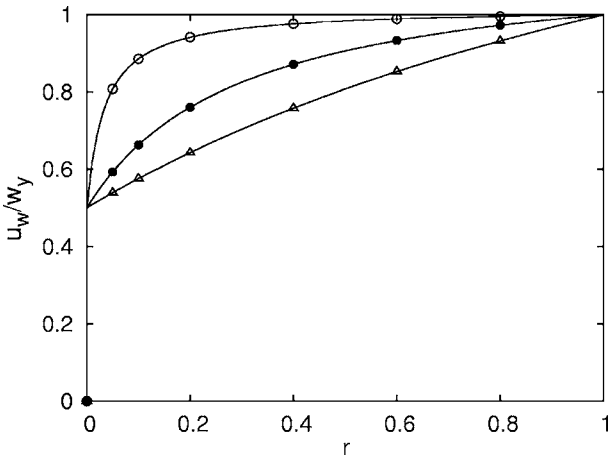

FIG. 3. Extrapolated fluid velocity u_w at the wall versus r for different values of τ; the distance of the wall is $a=0.7$. Simulated results are presented with empty circles for $\tau=1$, filled circles for $\tau=4$, and empty triangles for $\tau=10$. Analytical results are plotted with solid lines.

shown that this behavior results from the special choice of the interpolation in respect of the halfway position.

B. Moving square in a channel

To demonstrate the accuracy of the model for walls moving in both the x and y directions, periodic repetition of a square moving in the direction of its diagonal in a channel is simulated (Fig. 5). In an $N\times N$ domain the channel is considered as a square rotated by 45°. The boundary nodes at the channel walls and the inlet and outlet are defined along a fixed diagonal line of the Cartesian grid. At the channel walls (2) a linear interpolation scheme [5] (the wall crosses at half lattice spacing) is used; at the inlet and outlet (1) the periodic boundary condition is used. The solid square with size L and velocity $w_x=w_y=w$ moves along the centerline of the channel; on its walls the slip boundary condition proposed here is used. The position of the moving square is updated at each

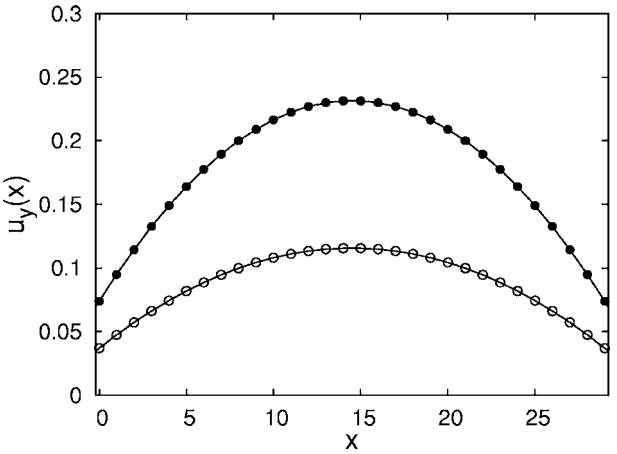

FIG. 4. Velocity profile of Poiseuille flow. The parameters are $\tau=2.5$, $r=0.4$, $a=0.2$; empty circles for $g=5e-4$; filled circles for $g=1e-3$; theoretical results are presented with solid lines.

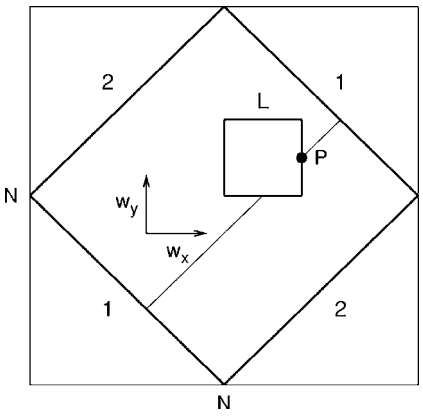

FIG. 5. Geometry of the moving square in a channel, the P point where the extrapolated slip velocity is measured, and the continuous path of P. (For even L the path is along a diagonal line of the grid; in this case the extrapolation involves the two nearest-neighboring fluid nodes lying on this path.)

time step according to its velocity. The computational algorithm is as follows. (1) Calculate the postcollision distribution functions, (2) carry out the streaming process, (3) rewrite the distribution functions at the boundary nodes using the appropriate boundary conditions (BCs), (4) calculate the new square position, and (5) calculate the macroscopic quantities. After the square has moved one lattice spacing, it is necessary to define distribution functions at the new boundary nodes appearing instantly behind the square. In this case we use a quadratic interpolation such that

$$f_i(\boldsymbol{x},t) = 3f_i(\boldsymbol{x}+\boldsymbol{e}\delta,t) - 3f_i(\boldsymbol{x}+2\boldsymbol{e}\delta,t) + f_i(\boldsymbol{x}+3\boldsymbol{e}\delta,t), \tag{23}$$

where $\boldsymbol{e}$ is the unit out-normal vector at the wall. A similar procedure is applied in Ref. [16]. The slip velocity, the difference between the tangential component of the fluid

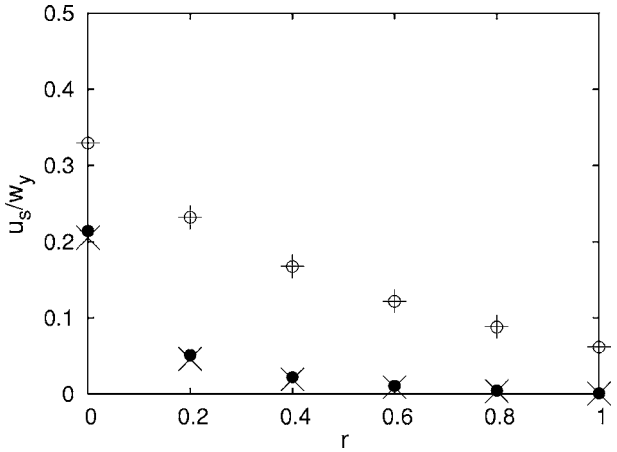

FIG. 6. Normalized slip velocity at P for the moving square; empty circles for $\tau=5$ and filled circles for $\tau=1$. The corresponding values of the slip velocity in the Galilean-invariant case are presented with + and ×.

velocity and w_y, is measured at a specified point (P) which is exactly at the center of the front side of the square. In general, this point lies between grid points; hence it is necessary to extrapolate the velocity from the surrounding values. In our case linear extrapolation is used. Figure 6 shows the steady slip velocity for different r, τ; other parameters are $N=100$, $L=20$, and $w=1e-3$. Figure 6 also shows the values of the slip velocity obtained from a simulation of the Galilean-invariant counterpart. In that case the same grid is used, the square is at rest $(w=0)$, and the channel walls move in the opposite direction with the same absolute velocity. The walls of the square are fixed at half lattice spacing from the last fluid node, Eq. (11)–(13) are applied as BCs with $w_y=0$, and the linear interpolation scheme on the channel walls is modified according to their movement. The agreement between the two situations is excellent. However, for larger velocities a correction is required. Several simulations have been performed at other parameters relating to the slip-flow regime $(0.01<Kn<0.1)$ and give the same result.

IV. CONCLUSION

To summarize, we have presented a kinetic-type boundary condition in the lattice Boltzmann method to model slip flow over straight walls placed at arbitrary positions. The momentum exchange at the wall is taken into account by varying the scattering kernel based on boundary-node collision rules in lattice gases. The special interpolation with respect to the halfway position gives a slip velocity that is independent of the wall position in first order of the Knudsen number. Numerical simulations of Couette and Poiseuille flows agree with the derived analytical results to machine order. A computer simulation of a square moving in the direction of its diagonal shows that the model provides accurate results dealing with walls moving in both the tangential and normal directions. This suggests that the method presented here is a valuable tool in modeling microflows or rarefied gases [6,10]. One of the potential extensions of the model is a boundary treatment on curved interfaces, which is currently in progress by the author and will be reported in the future.

[1] U. Frisch, B. Hasslacher, and Y. Pomeau, Phys. Rev. Lett. **56**, 1505 (1986).
[2] X. He and L. S. Luo, Phys. Rev. E **56**, 6811 (1997).
[3] Q. Zou, S. Hou, and G. D. Doolen, J. Stat. Phys. **81**, 319 (1995).
[4] H. Chen, C. Teixeira, and K. Molvig, Int. J. Mod. Phys. C **9**, 1281 (1998).
[5] M. Bouzidi, M. Firdaouss, and P. Lallemand, Phys. Fluids **13**, 3452 (2001).
[6] X. Nie, G. D. Doolen, and S. Chen, J. Stat. Phys. **107**, 279 (2002).
[7] L. Zhu, D. Tretheway, L. Petzold, and C. Meinhart, J. Comput. Phys. **202**, 181 (2005).
[8] G. H. Tang, W. Q. Tao, and Y. L. He, Phys. Fluids **17**, 058101 (2005).
[9] Y. H. Zhang, R. S. Qin, Y. H. Sun, R. W. Barber, and D. R. Emerson, J. Stat. Phys. **121**, 257 (2005).
[10] D. L. Morris, L. Hannon, and A. L. Garcia, Phys. Rev. A **46**, 5279 (1992).
[11] M. Sbragaglia and S. Succi, Phys. Fluids **17**, 093602 (2005).
[12] P. L. Bhatnagar, E. P. Gross, and M. Krook, Phys. Rev. **94**, 511 (1954).
[13] S. Chen and G. D. Doolen, Annu. Rev. Fluid Mech. **30**, 329 (1998).
[14] A. J. C. Ladd, J. Fluid Mech. **271**, 285 (1994).
[15] X. He, Q. Zuo, L. S. Luo, and M. Dembo, J. Stat. Phys. **87**, 115 (1997).
[16] P. Lallemand and L. S. Luo, J. Comput. Phys. **184**, 406 (2003).